Solar Energy Materials and Solar Cells 179 (2018) 31–35

Contents lists available at ScienceDirect

Solar Energy Materials and Solar Cells

journal homepage: www.elsevier.com/locate/solmat

Automated detection of rear contact voids in perc cells with photoluminescence imaging

Kortan Öğütman[a,c,d,*], Kristopher O. Davis[a,c], Haider Ali[a,c,e], Steven R. Martell[f], Winston V. Schoenfeld[a,b,c,d,e]

[a] Florida Solar Energy Center, University of Central Florida, Cocoa, FL 32922, USA
[b] CREOL, the College of Optics and Photonics, University of Central Florida, Orlando, FL 32816, USA
[c] c-Si Division, US Photovoltaic Manufacturing Consortium, Orlando, FL 32826, USA
[d] Dept. of Electrical Engineering and Computer Science, University of Central Florida, Orlando, FL 32816, USA
[e] Dept. of Materials Science and Engineering, University of Central Florida, Orlando, FL 32816, USA
[f] SONOSCAN, Inc., 2149 E. Pratt Blvd., Elk Grove Village, IL 60007, USA

ARTICLE INFO

Keywords:
Photoluminescence
PERC cells
Voids
Recombination
Acoustic microscopy

ABSTRACT

An image-processing method combined with Fourier analysis is introduced in this work as a rapid and highly-automated method of detecting rear contact voids in passivated emitter and rear contact cells (PERC). This approach utilizes photoluminescence (PL) imaging to locate the central point of the most detrimental type of voids and associate a void fraction to each cell in a manner of seconds. Acoustic microscopy and scanning electron microscopy are also used as complementary tools to confirm the presence of voids detection using PL imaging and provide more insight into the actual physical mechanism of what is observed in PL measurements.

1. Introduction

As the transition from standard full area aluminum back surface field (Al-BSF) cells to PERC becomes more pronounced, the need for industrially applicable and possibly in-line characterization of PERC cells turns out to be a relevant task. PERC cells lead to higher conversion efficiencies due to lower surface recombination and better light trapping. These are achieved by incorporating a passivating dielectric stack at the rear surface and locally opened rear contacts, instead of a full-area BSF and Al back contact. The insertion of the dielectric layers provides a higher open-circuit voltage and improves the long-wavelength response of the cell by increasing the back-reflectance [1]. This structure is expected to gain major market share and practical roadmaps show the possibility of reaching efficiency values of 22% in high-volume manufacturing [2].

One possible challenge, as the carrier transport becomes two or three-dimensional for line and dot contacts, respectively, is the decrease in fill factor due to higher series resistance [3]. Another problem that has widely occurred during the production of these cells is the formation of voids around the local contacts [1,4,5]. This can be attributed to the Kirkendall effect, which governs the diffusion of atoms through vacancies. The formation of voids can be explained by several factors. As it was shown by the earlier work, as the contact spacing increases, the diffusion of the silicon atoms from the bulk to the aluminum matrix will become more likely [5]. This will also lead to a decrease in the thickness of the local back-surface field. Analysis from the same work also showed that, when there is a eutectic layer formed, silicon content in the Al-matrix diminishes, and instead the silicon from the Al-Si melt recrystallizes to form the BSF. This may lead to a void with BSF. Therefore, if the contact spacing is too large, there may not be enough silicon in aluminum to form the eutectic layer, which then could lead to a void without BSF. High diffusive behavior of silicon is alleviated by introducing Si into the paste prior to alloying, which will lead to higher silicon content in the Al-Si melt for better eutectic formation [5]. Furthermore, recent studies also suggested that the Kirkenall effect may not be the ultimate cause of void formation after all. Dressler et al. illustrated that, by tweaking the time intervals for both cooling and heating, the trend for void formation stay the same, which refutes the existence of Kirkendall effect [6]. Kranz *et al.* concluded, by measuring the thickness of BSF, that void formation takes places during the recrystallization while Al is still in the liquid phase. From there, it was observed that contact height influences the interaction between the Al-Si melt and silicon surface itself, the larger the contact height the smaller wetting of the silicon surface by the Al-Si melt [7]. Voids without the BSF will turn out to be the most detrimental ones in terms of effecting solar cells' conversion efficiency [4]. This is due to minority carriers not being shielded by the back-surface field and causing increased recombination at the rear side of the cell. This type of void will

---

[*] Corresponding author at: Florida Solar Energy Center, University of Central Florida, Cocoa, FL 32922, USA.

https://doi.org/10.1016/j.solmat.2018.02.009
Received 6 July 2017; Received in revised form 8 January 2018; Accepted 6 February 2018

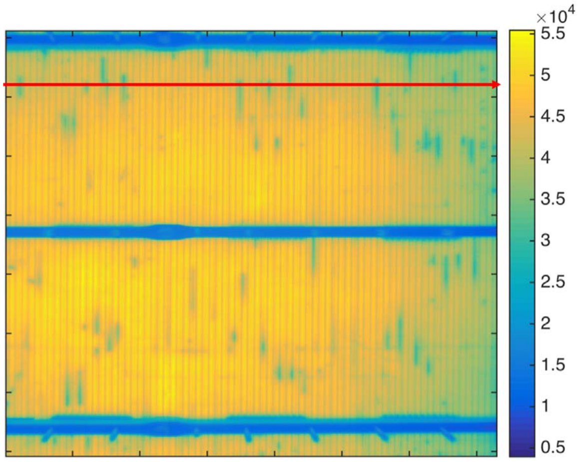

Fig. 1. Open-circuit PL image of a PERC cell that has numerous voids.

also cause increased series resistance since majority carriers need longer distances to reach a healthy contact to be extracted out of the solar cell.

A number of research groups came up with different detection mechanisms to detect voids. Urrejola et al. [8] provided the very initial study concerned with why the voids might be formed in PERC cells with the aid of energy dispersive x-ray spectroscopy EDS/EDX analysis. Dressler et al. used acoustic microscopy (AM) to illustrate the existence of voids combined with electroluminescence (EL) measurements [9]. As shown in [5], AM and EL analysis demonstrated that not all voids impact the cell performance in a significant way. Recently, Großer et al. utilized light-beam induced current (LBIC) quantify the electrical losses associated with void-related features, along with assigning an area fraction due to electrically active voids [10]. Given these previously published methods, a fast and reliable way of distinguishing recombination-active voids proves to be a relevant task. In this work, we present an automated way of detecting the most detrimental type of voids in a manner of seconds using open-circuit PL imaging in combination with our image-processing technique. In addition to this, we explore the nature of the using a combination of PL, AM and SEM imaging techniques conducted on the same sample.

2. Methodology

PL intensity is a sensitive way of detecting local voltage values along the cell, which scales with intrinsic carrier concentration and the related constants, as shown below [11].

$$I_{PL} = \exp\left(\frac{V_{oc}\bullet q}{k\bullet T}\right)\bullet A_i\bullet B\bullet {n_i}^2 \tag{1}$$

where q is the elementary charge, k is the Boltzmann constant, T is temperature , A_i is a scaling factor, and B is the radiative recombination coefficient for silicon. Due to the relationship between the local voltage and the recombination current [12], and given the high-resolution PL imaging systems currently available, PL imaging is particularly well-suited for detecting the recombination-active voids in PERC cells [13]. An example of an open-circuit PL image for a PERC cell with voids is shown in Fig. 1.

Within the framework of this paper, we develop an image-processing technique that automatically detects these highly detrimental voids, which lack both a BSF and eutectic layer. To do so, we start by analyzing a line-scan taken perpendicular to the linear local back contacts of the PERC cells used in this study, as highlighted by the red line in Fig. 1 The inverse of PL intensity is then calculated, where peaks in the line scan correspond to regions with a low PL intensity, as shown in Fig. 2(a). Here, it is difficult to distinguish the intensity reduction due to the front contact fingers, which are parallel to the linear local back contacts. To address this, we take advantage of the fixed spatial frequency ($\approx$1 mm or $\approx$10 pixel counts) of these front contact fingers. A Fourier transform is then performed on the inverse PL intensity to isolate the aforementioned frequency component and a cut-off filter is applied to remove these features. Following this step, a MATLAB-based image processing algorithm is used for the detection of the voids present in the PL image along with characteristics of the voids like their width and prominence, as shown in Fig. 2(b).

Quite significantly, the presence of front contact fingers can be eliminated from the analysis and void features can be isolated as a result of this procedure, as shown by the blue arrows in Fig. 2(b). To transform this detection procedure to the whole cell, one can repeat this analysis for each row of pixels in the PL image. By doing this, and image of the voids can be created for the cell. Since the actual size of the linear local back contacts is known by the manufacturer ($\approx 60\,\mu m$, in this case), the localization of the central point of void can be used to calculate a void fraction for the cell of interest as well.

3. Experimental details

In this work, we use industrial scale PERC cells, made from 156 mm × 156 mm *p*-type Cz wafers with a thickness of $\approx$180 µm. The cells were made using standard processes and feature linear local back contacts with a width of 60 µm and pitch of $\approx$1 mm. A BT Imaging LIS-R1 system with an 808 nm laser excitation source was used to collect one sun open-circuit PL images. One sun was established by adjusting the laser intensity until the short-circuit current density measured with

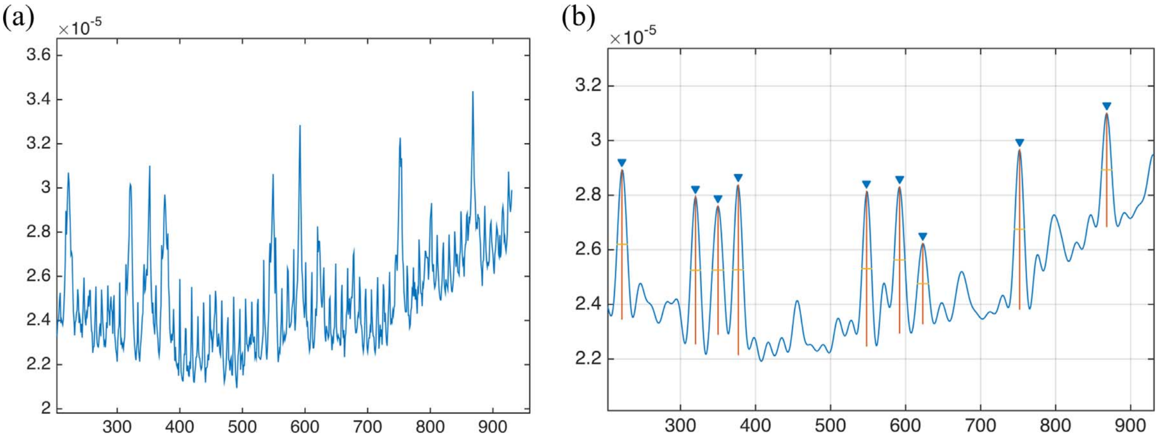

Fig. 2. (a) Example of an inverse PL line scan taken perpendicular to the linear local back contacts for the PERC cell shown in Fig. 1. (b) The same line scan following a high-pass filtering process and feature detection step. The features with blue arrows above them indicate voids.